Inorganica Chimica Acta 502 (2020) 119354

Contents lists available at ScienceDirect

Inorganica Chimica Acta

journal homepage: www.elsevier.com/locate/ica

Research paper

Synthesis of vinyl-terminated HDPE and PE/xGnP composite using dinuclear Co-based catalyst

Enayat Rahimipour[a], Gholamhossein Zohuri[a,*], Mahsa Kimiaghalam[a], Mostafa Khoshsefat[b]

[a] Department of Chemistry, Faculty of Science, Ferdowsi University of Mashhad, P.O. Box: 91775, Mashhad, Iran
[b] Key Laboratory of Engineering Plastics, Beijing National Laboratory for Molecular Sciences, Institute of Chemistry, Chinese Academy of Sciences, Beijing 100080, China

ARTICLE INFO

Keywords:
Ethylene polymerization
Late transition metal catalysts
Multinuclear catalysts
Methylaluminoxane
Nano-composites

ABSTRACT

To continue our previous researches on dinuclear late transition metal catalysts, a dinuclear catalyst based on cobalt (C) was prepared and used for polymerization of ethylene in the presence of modified methylaluminoxane (MMAO) as cocatalyst. The behavior of catalyst C was compared with its mononuclear analogue (M). The initial results showed higher in both activity and stability of the catalyst C in comparison to catalyst M. Based on this, the studies were focused on the catalyst C. The maximum activity of C observed at [Al]/[Co] molar ratio of 2000:1, reaction temperature of 60 °C that was equal to 6.8 × 10^6 g PE/mol Co.h. The GPC-IR results showed that the synthesized polyethylene has low M_w (M_w = 7.0 × 10^3 g/mol) along with a narrow MWD (2.56). Moreover, the polyethylene was containing low SCB (7.8 CH_3/1000C) in confirmation of high crystallinity obtained by DSC (χ_c = 60%). Due to layered morphology of the catalyst C observed through SEM images, the shape of PE was layered consistent on replication phenomenon. Besides, this morphology observed in SEM and TEM images of PE/xGnP composites with higher intensity. The presence of xGnP also led to a slightly greater activity of the catalyst C along with higher vinyl content and lower starting degradation temperature of the obtained PE.

1. Introduction

What is expected from multinuclear catalysts in comparison to mononuclear analogues includes better performance and selectivity [1–3]. This great performance can be achieved through adjacency of the centers [2,4–7]. In some reports, both factors (i.e. activity and selectivity) have improved while within the others, one of them has shown better results [8]. It should be noted that for multinuclear catalysts, it is desirable to have cooperative effects for production of advanced polyolefin materials. The cooperative and multinuclearity effects afford greater monomer insertion and therefor catalyst activity, consequently, through increasing local concentration of (co)monomers and sacrificial impact [2,8]. Besides, monomer reconfiguration and co/macro(monomer) supply by the second center could generate a new microstructure or decrease the need for using comonomer or even impact modifier [9]. This fact demonstrates that the nature of centers is as important as the number of them. All these are considerable if the centers posed in an effective distance. Moreover, steric and electronic effects of the bridge can control and modulate cooperative effects [2,4,10–13].

Although there are many papers on catalyst for olefin polymerization, nowadays, the share of reports on the catalysts based on Fe, Co, Ni and Pd is too much due to unique and attractive pattern along with convenience in synthesis [14–18]. On the other hand, regulation of the catalyst activity through ligand modification and production of HDPE or α-olefin with very high turnover frequency are some characteristics of Fe or Co based catalysts [17–19]. Activity of these catalysts is competitive to Ziegler-Natta and metallocene catalysts. Some notable examples on homo- and hetero-structure on Co and Fe are described as following. J. Sun et al. has reported dinuclear bis(imino) pyridine iron based catalysts bearing methylene bridge activated by TiBA that produced HDPE with higher molecular weight and even better performance [20]. These observations were in comparison to the mononuclear catalysts. The steric and electronic effects of the dinuclear structures are the reasons of the higher performance. Trinuclear Fe/Ni complex of bis(imino)pyridine/α-diimine based ligand reported by Kim et al. has showed higher catalytic activity and longer life time than related monometallic Ni and homo-bimetallic Fe complexes proving synergistic effect due to the neighboring of the metal centers [21]. T. Sun and co-workers have prepared heterobinuclear cobalt and nickel complex, with ligand containing α-diimine and pyridine diimine moieties [22]. Activity of the heterobinuclear complex

* Corresponding author.
E-mail address: zohuri@um.ac.ir (G. Zohuri).

https://doi.org/10.1016/j.ica.2019.119354
Received 1 November 2019; Received in revised form 9 December 2019; Accepted 9 December 2019
Available online 11 December 2019
0020-1693/

were lower than binary catalyst system and corresponding mononuclear complexes. Additionally, metal centers in the heterobinuclear complex is selectively could be activated by different cocatalysts [22]. Dinuclear cobalt based catalysts containing bis(phenyl) bridge between the centers have reported by W.H. Sun et al. where the higher activity, thermal stability and lifetime than mononuclear analogues have observed [23]. The obtained PE was linear and MWD of the samples were in a broad range. Moreover, some methylene-bridged structures were prepared by this group exhibiting high activity in production of vinyl-terminated PE waxes [24]. Bianchni et al. have synthesized dinuclear Fe and Co based catalysts bearing 2,6-bis iminopyridine structures [25]. These asymmetric structures have been activated by MAO, have shown good activity in oligomerization of ethylene and higher α–olefins. Depending on type and number of centers, high selectivity and Schultz-Flory distribution has obtained. Activity of the catalysts was four times greater than the mononuclears regarding the coordination of nitrogen to cobalt metal atoms. Takeuchi's group research has reported a series of dinuclear cobalt (double-decker framework) species affording higher molecular weight of PE than mononuclear analogue with a moderate activity [26]. Several one side shielded (low steric effect) dinuclear complexes have synthesized by different research groups affording oligomer to mixture of oligomer/polymer which the activities were moderate to high [27–32].

One the other side, α-diimine structures bearing isopropyl substituents on the side aryl rings and methyl groups on the phenyl linker have been investigated by our group that showed high activity in polymerization of both ethylene and α–olefins [2,33]. The same bridges have used in synthesis of bis (imino) pyridine dinucear Fe-based catalysts where the catalyst bearing optimum bulkiness (isopropyl and methyl) around the active center showed the highest activity among the studied structures [10]. Moreover, high crystallinity of polyethylene obtained by the catalyst. Based on this, the same ligand structure, herein, was used in synthesis of cobalt based catalyst and employed in polymerization of ethylene in presence of MMAO as cocatalyst. The performance of the catalyst C was comprised with its mononuclear analogue. The effect of polymerization parameters was examined on the catalyst behavior. Additionally, the influence of exfoliated graphene nanoplatelet (xGnP) was investigated as nanocarbons especially graphene nanoplatelets have impacts on catalyst behavior and polymer properties [34,35].

2. Experimental

2.1. Materials

All experiments were performed under an atmosphere of dry argon using standard Schlenk techniques. Toluene was distilled under argon from sodium/benzophenone immediately prior to use. Methanol (Merck Chemical) was purified by heating over iodine activated magnesium with a magnesium loading of 0.5–5.0 g/L and distilled before use in complex and ligand synthesis as solvent. Polymerization grade ethylene gas (purity 99.9%) (Iran, Petrochemical) was purified by passing through activated 4 Å/13X molecular sieves column. 2,6-Diacetylpyridine, 2,6-diisopropyl aniline, 2,3,5,6-trtramethyl-1,4-phenylene diamine, cobalt (II) chloride (purity 97%) and diethyl ether and *n*-hexane (purity 99.5%) were supplied by Merck Chemical (Darmstadt, Germany) and used in synthesis of ligands and catalysts. Decalin (purity 97%), chlorobenzene, and calcium hydride were purchased from Sigma Aldrich Chemicals (Steinheim, Germany). Triisobutylaluminum (purity 93%) was supplied by Sigma Aldrich Chemicals (Steinheim, Germany) which was used in synthesis of MMAO according to the literature [15]. Ethylene polymerizations were conducted in a 1-L stainless steel Buchi bmd 300-type stainless steel reactor, using toluene as solvent. The reactor was purged with nitrogen at 90 °C for 2 h prior to each reaction. Toluene, cocatalyst and catalyst were introduced under nitrogen atmosphere, respectively. The reactor was saturated with ethylene to desired total pressure and reaction proceeded at different conditions by mixing at 800 rpm. Finally, the reactor was evacuated and the product was washed with acidic methanol (5%) and dried under reduced pressure. *In-situ* polymerization was performed by introduction of xGnP (1.7–2 nm thickness or grade M supplied by XG Sciences, East Lansing, USA) premixed with cocatalyst.

2.2. Characterization

^{1}H NMR and FT-IR spectrums were obtained using Bruker AC-300 and Thermo Nicolet AVATAR 370 spectrometers, respectively. Elemental analysis was performed on a Thermo Finnigan Flash 1112EA microanalyzer. Vinyl content of the polymer samples were determined according to the method described elsewhere [36]. The viscosity average molecular weight (M_v) of the polymer samples was determined according to the literature using an Ubbelohde viscometer [15]. Molecular properties of the PE sample were determined with a Polymer Char high-temperature gel permeation chromatographer (GPC), run at 145 °C under a flow rate of 1,2,4-trichlorobenzene of 1 mL min^{-1}. The GPC was equipped with three detectors in series (infrared, light scattering, and differential viscometer) and calibrated with polystyrene narrow standards. Differential scanning calorimetry (DSC) thermograms were recorded at second heating cycle with the rate of 10 °C/min by Perkin Elmer DSC Q100 instrument. Successive self-nucleation and annealing (SSA) analysis was carried out at the heating and cooling rates of 10 °C min^{-1}. Samples were first heated to 180 °C, maintained for 10 min, and cooled down to 25 °C. Subsequently, samples were heated to the first self-nucleation temperature (T1), maintained for 10 min then cooled down to 25 °C. Successive self-nucleation was achieved by repeatedly heating to the next self-nucleation temperatures and cooling down to 25 °C. After covering the temperature range between 165 and 25 °C, the final heating ramp from 25 up to 170 °C was applied to collect all melting endotherms. SEM and TEM images were obtained by LEO 1450VP and Philips CM12 instruments, respectively. Thermogravimetric and differential thermogravimetric curves were extracted from Perkin Elmer TGA-7 equipment which the analyses were carried out at a rate of 10 °C min^{-1}.

2.3. Synthesis of ligand and catalyst

The molecular structures of mono- and dinuclear catalysts (M and C) are depicted in Fig. 1. The ligand and corresponding mononuclear catalyst M were prepared according to our previous reports [37,38]. However, ligands L_1 and L_2 and corresponding dinuclear precatalyst C were synthesized according to a modified procedure described in our recent paper except $FeCl_2$ replaced with $CoCl_2$ [10,39]. More details on modified method and characterization are provided in supporting information (SI).

3. Results and discussion

3.1. Effect of polymerization parameters on the catalyst behavior

To optimize the polymerization parameters, reactions were carried out at different condition. [Al]/[Co] molar ratio (MMAO as cocatalyst) showed an optimum value at 2000:1 where the catalyst activity increased from 3.8 to 5.3 × 10^6 grPE/mol Co.h, due to reaching the highest concentration of active centers [2,15,40]. This value then decreased to 3.2 × 10^6 grPE/mol Co.h that may attribute to the formation of inactive species at higher concentration of the cocatalyst [2,10,15,33]. In comparison to mononuclear catalyst M, activity of the dinuclear catalyst C was greater in all studied range of cocatalyst concentrations (i. e. 500 to 2500). These observations were consistent on our previous results on mono and dinuclear catalyst based on Fe [10] (Fig. 2).

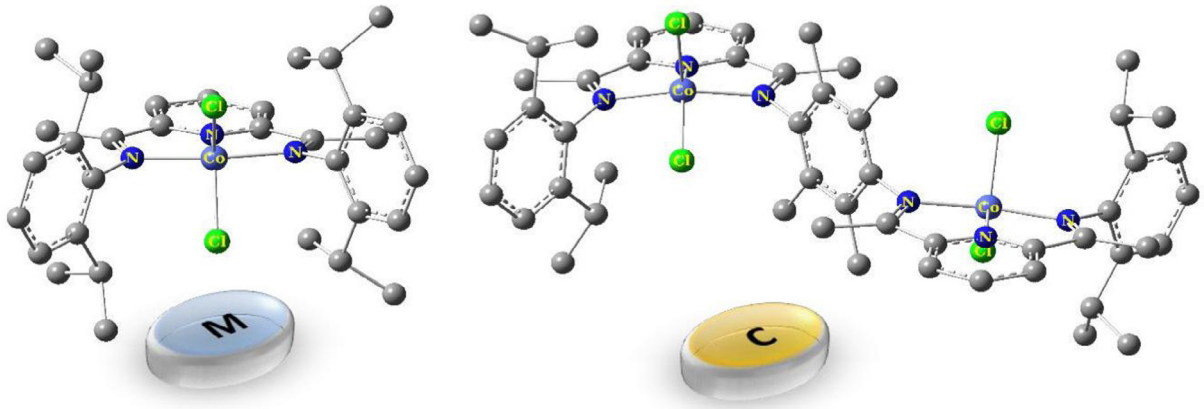

Fig. 1. Molecular structures of mononuclear (M) and dinuclear (C) catalysts. Hydrogen atoms have been omitted for clarity.

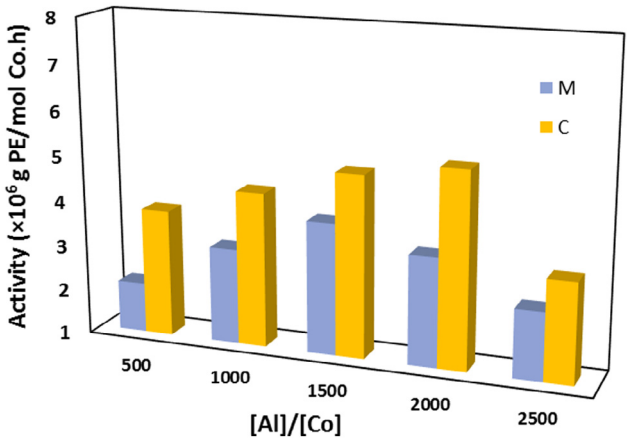

Fig. 2. Comparison of results of ethylene polymerization at different [Al]/[Co] molar ratios using mono and dinuclear catalysts (M and C).

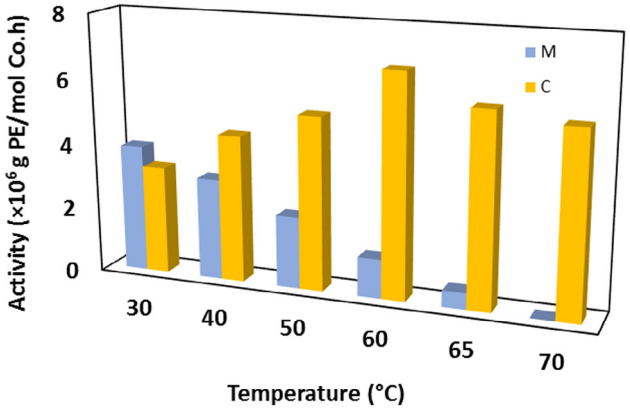

Fig. 3. Comparison of results for ethylene polymerization at different temperatures using the mono and dinuclear catalysts (M and C).

The effect of polymerization temperature exhibited the stability of the catalyst complex up to 70 °C that is a characteristic for the dinuclear catalyst C. However, the greatest activity of the polymerization was obtained at 60 °C in the range studied (50–70 °C) for C. In contrast, the trend for the catalyst M was descending as the polymerization temperature was raised. In this point of view, the dinuclear catalyst C is much more stable than the catalyst M (Fig. 3). Physical factors such as higher kinetic energy of polymerization species led to great interaction and reaction rate affording better performance of the catalyst

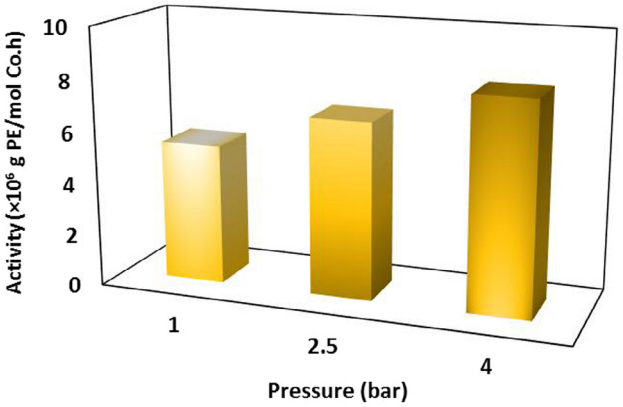

Fig. 4. Effect of monomer pressure on polymerization using the dinuclear catalyst C.

Table 1
Properties of PE made by dinuclear catalyst C at different polymerization temperatures and time.[a]

Entry	t_p (min)	T_p (°C)	T_m[b] (°C)	X_c[b] (%)	$\bar{M}_v$[c] ($\times 10^4$ g.mol^{-1})	Vinyl content[d]
1	40	60	128.2	63	4.8	10.4
2	40	65	125.8	60	3.2	11.6
3	40	70	125.0	54	2.6	17.4
4	20	60	125.6	53	0.3	9.1
5	60	60	125.0	61	4.8	11.9

[a] Condition: [Co]: 5 μmol, [Al]/[Co]:1000:1, ethylene pressure: 2.5 bar, toluene 35 mL.
[b] Obtained by DSC.
[c] Obtained by Ubbelohde Viscometer.
[d] Obtained by FT-IR spectrometer.

[10,15,41]. In contrast, catalyst deactivation and decreasing of monomer solubility are the chemical and physical factors for dropping the catalyst activity at higher temperatures [10,15,41].

Due to less activity of the mononuclear catalyst M, further studies were focused on the catalyst C. Based on this, activity of the catalyst C also affected by monomer pressure as the ethylene concentration augmented in the reactor (1–4 bar). Higher concentration of the monomer surrounding the active centers and increasing of polymerization rate caused higher level of activity [10] (Fig. 4).

Polymerization at prolonged time (according to the kinetic profile provided in SI; Fig. S1) revealed that the catalyst is active even after 40 min of the polymerization. Well interaction of catalyst-cocatalyst for

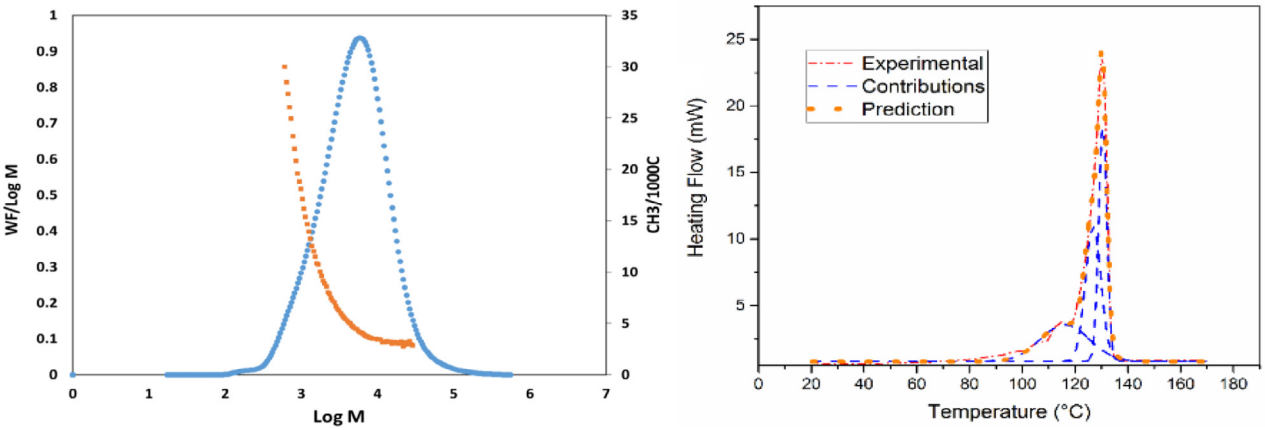

Fig. 5. GPC-IR (left) result and SSA thermogram (right) of PE made by the catalyst C (entry 2).

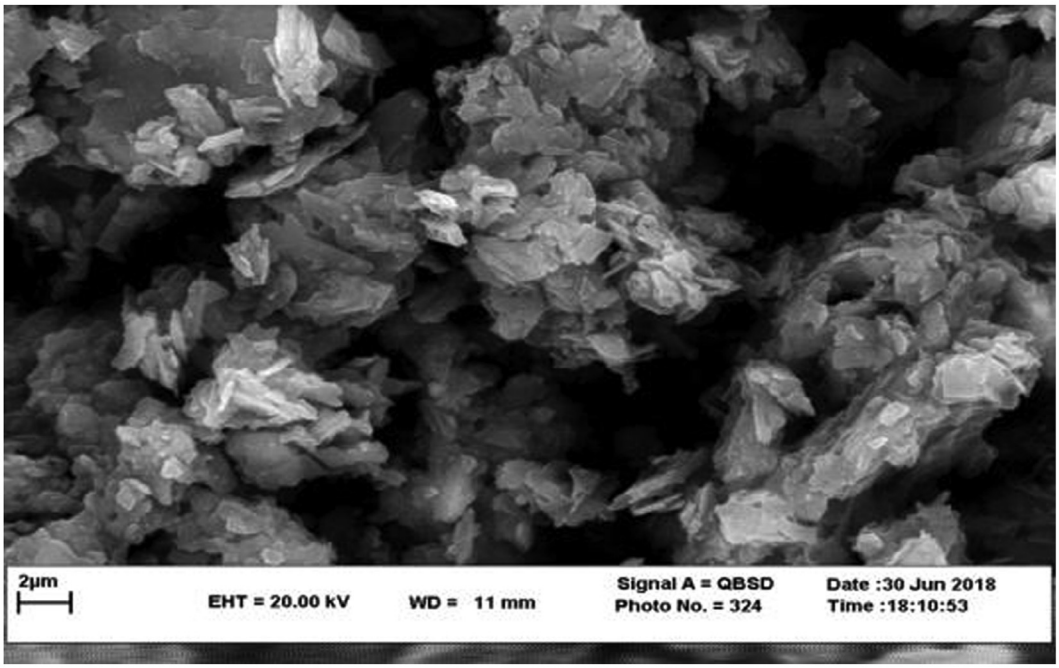

Fig. 6. SEM image of the catalyst C (10000x).

reactivation of active center is important for the observed catalyst behavior. Irreversible catalyst deactivation is the main reason for decreasing of the activity by time [10,15].

3.2. Effects of polymerization parameters on the microstructural and thermal properties of the polymer

Polymerization temperature as an effective factor on the catalyst behavior and polymer properties showed that crystallinity along with melting point decreased as temperature of the reaction raised. These observations are due to increasing of chain transfer reaction and short chain branch (SCB) formation leading to thinner crystalline domains and lamellae [2,10,42]. High crystallinity and melting point along with low SCB are the characteristics of HDPE that observed for the samples through different methods. In addition to thermal properties, viscosity average molecular weight ($\bar{M}_v$) of the samples decreased as chain transfer and termination reactions increased by temperature [15,38,41,42]. The results were along with the increasing of the vinyl content of the polymer chains (according to Fig. S2). In addition to the polymerization temperature, reaction time also showed a strong impact on the polymer properties. As it can be observed in Table 1, crystallinity of the PE samples increased with polymerization time. The same trend was observed for $\bar{M}_v$. These can be attributed to the growth of polymer chain and increasing of methylene sequences. An optimum value was observed for vinyl content of the polyethylene chain. It may ascribe with vinyl end polymer chains consumption by active centers or β–H eliminations at different stages of the polymerization. The mechanism from activation to termination has explained elsewhere [10].

The GPC-IR result of entry 2 showed that the synthesized PE has low $\bar{M}_w$ ($\bar{M}_w = 7.0 \times 10^3$ g/mol) along with a narrow MWD (2.56) (Fig. 5(right)). Moreover, the polyethylene was containing low SCB (7.8 CH_3/1000C) in confirmation of high crystallinity obtained by DSC. In the other side, there are some contributions at the temperatures higher than 110 °C revealing low SCB and long methylene sequences for the sample (Fig. 5(left)).

3.3. Effect of xGnP on catalyst behavior and PE properties

To investigate the effect xGnP, very low amount of xGnP (i. e. 7 mg) was premixed with cocatalyst and introduced to the reactor before injection of the catalyst [33]. Initial results showed a slight increasing of

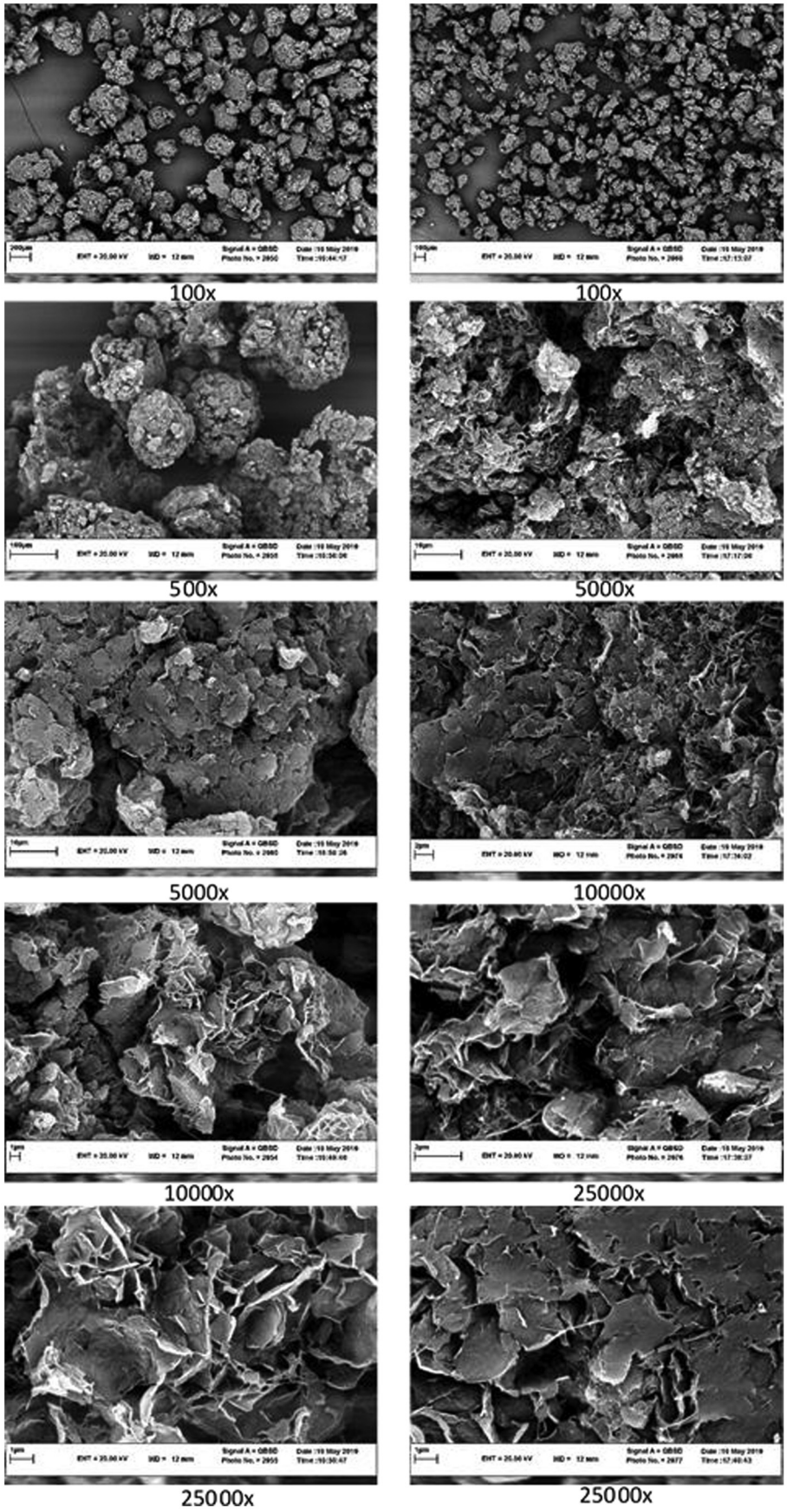

Fig. 7. SEM images of the PE sample (left) and PE/xGnP composites made by the catalyst C (right).

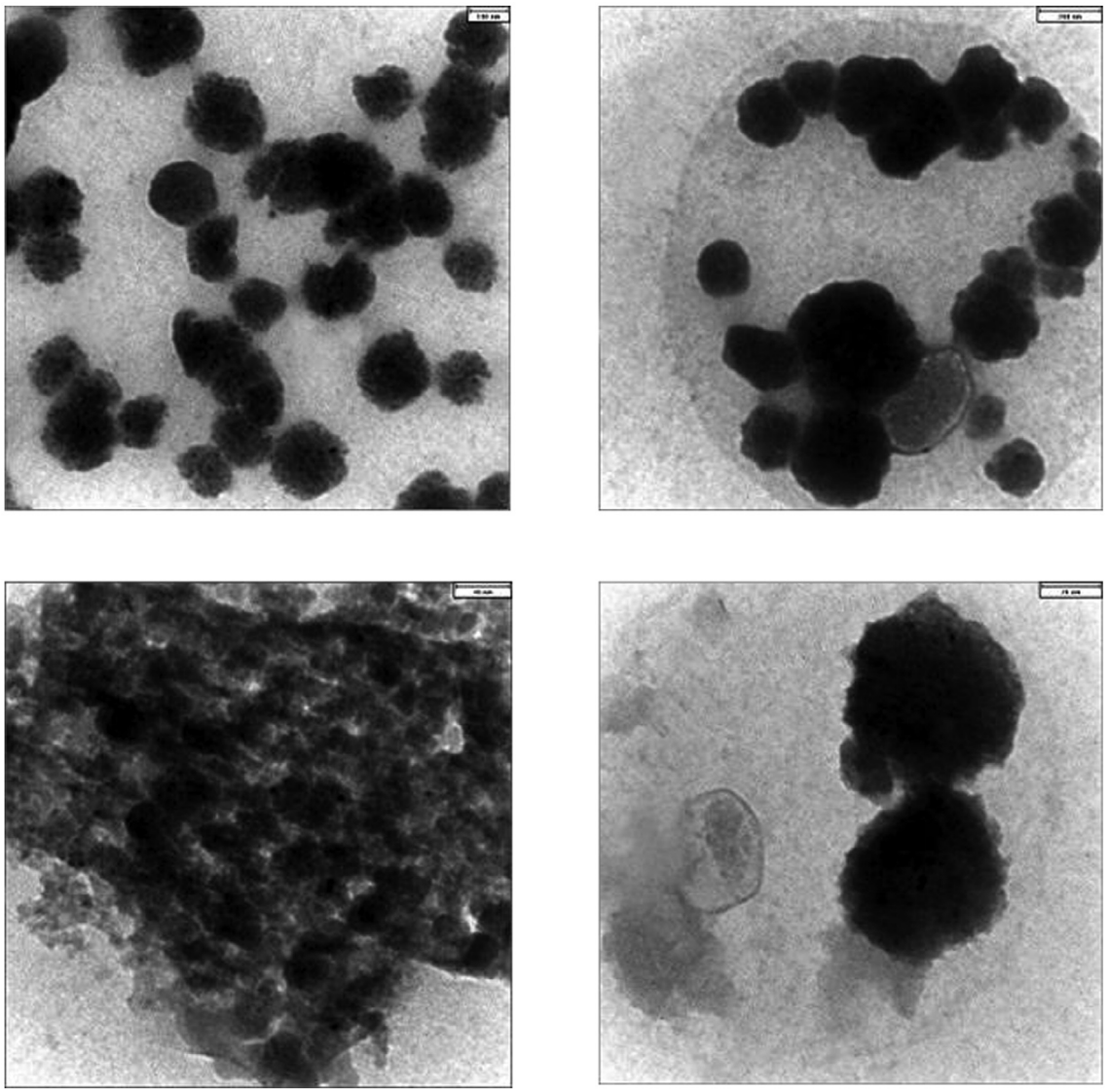

Fig. 8. TEM images of PE/xGnP composite made by the catalyst C.

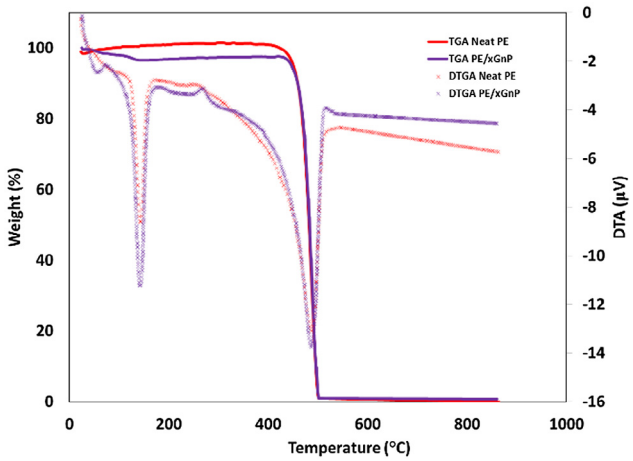

Fig. 9. TGA and DTGA curves of neat PE and PE/xGnP samples.

the catalyst activity up to 7.0 × 10^{6} g PE.mol^{-1}.h^{-1}. However, the effect of xGnP on PE properties was much more interesting and striking. As it can be observed in Fig. S3, vinyl content of the PE/xGnP sample is higher than neat PE. SEM image of the catalyst C (Fig. 6) exhibited a layered morphology of the catalyst particles which also can be observed in the produced PE at different stage of the polymerization (Fig. 7 (left)). It is suggested that morphology of the polymer particles replicate from the shape of the catalyst particle. The effect of xGnP on morphology of the polymer particles depicted in Fig. 7 (right). The SEM images at different magnification from 100× to 25,000× demonstrates that the layered morphology of the polyethylene particles increased in presence of xGnP. TEM images also confirmed well dispersion of the xGnP in the polyethylene phase (Fig. 8).

Results of thermogravimetric analysis of the neat PE and composite can be observed in Fig. 9. According to the curves, degredation of PE initiates at lower temperature in presence of xGnP due to high thermal conductivity of the graphene nanoplatelets. Moreover, weight lose of the samples was greater than neat PE due to mentioned reason. Besides, the morphology of the samples is effective for the observed properties.

4. Conclusion

The dinuclear catalyst based on Co (C) showed higher activity and stability than its mononuclear analogue (catalyst M) which could be due to dinuclearity and optimum bulkiness around the active centers.

The catalyst C also afforded PE with low $\bar{M}_w$ and narrow MWD. Due to low SCB of the polymer chain, the crystallinity of PE samples was high which are characteristics of HDPE. Polymerization parameters were effective on the catalyst behavior and PE properties. Another characteristic of the catalyst was layered morphology dedicating to the obtained PE according to replication phenomenon. The effect of xGnP, beside, was striking as the layered morphology of the PE improved and vinyl content of the sample was increased. While thermal properties of the PE such as initiating temperature of degradation decreased and weight loss of the polymer increased due to high conductivity of the xGnP.

CRediT authorship contribution statement

Enayat Rahimipour: Investigation, Writing - original draft. **Gholamhossein Zohuri:** Supervision. **Mahsa Kimiaghalam:** Methodology. **Mostafa Khoshsefat:** Conceptualization, Methodology, Visualization, Writing - review & editing.

Declaration of Competing Interest

The authors declare that they have no known competing financial interests or personal relationships that could have appeared to influence the work reported in this paper.

Acknowledgments

The authors are thankful of Ferdowsi University of Mashhad and Iran Polymer and Petrochemical Institute (IPPI) for all their cooperation.

Funding

This work was supported by Ferdowsi University of Mashhad (FUM, project code: 46118).

Appendix A. Supplementary data

Supplementary data to this article can be found online at https://doi.org/10.1016/j.ica.2019.119354.

References

[1] C.J. Stephenson, J.P. McInnis, C. Chen, M.P. Weberski, A. Motta, M. Delferro, T.J. Marks, ACS Catal. 4 (2014) 999–1003, https://doi.org/10.1021/cs500114b.
[2] M. Khoshsefat, A. Dechal, S. Ahmadjo, S.M.M. Mortazavi, G. Zohuri, J.B.P. Soares, Appl. Organomet. Chem. 33 (2019) e4929, , https://doi.org/10.1002/aoc.4929.
[3] M.R. Salata, T.J. Marks, Macromolecules 42 (2009) 1920–1933, https://doi.org/10.1021/ma8020745.
[4] S. Liu, A. Motta, A.R. Mouat, M. Delferro, T.J. Marks, J. Am. Chem. Soc. 136 (2014) 10460–10469, https://doi.org/10.1021/ja5046742.
[5] H. Li, T.J. Marks, Proc. Natl. Acad. Sci. U. S. A. 103 (2006) 15295–15302, https://doi.org/10.1073/pnas.0603396103.
[6] S.K. Noh, J. Lee, D.H. Lee, J. Organomet. Chem. 667 (2003) 53–60, https://doi.org/10.1016/S0022-328X(02)02125-3.
[7] S. Jüngling, R. Müllhaupt, H. Plenio, J. Organomet. Chem. 460 (1993) 191–195, https://doi.org/10.1016/0022-328X(93)83145-L.
[8] M. Delferro, T.J. Marks, Chem. Rev. 111 (2011) 2450–2485, https://doi.org/10.1021/cr1003634.
[9] J.P. Mcinnis, M. Delferro, T.J. Marks, Acc. Chem. Res. 47 (2014) 2545–2557, https://doi.org/10.1021/ar5001633.
[10] M. Khoshsefat, A. Dechal, S. Ahmadjo, S.M.M. Mortazavi, G. Zohuri, J.B.P. Soares, Eur. Polym. J. 119 (2019) 229–238, https://doi.org/10.1016/j.eurpolymj.2019.07.042.
[11] L. Guo, S. Dai, X. Sui, C. Chen, ACS Catal. 6 (2015) 428–441, https://doi.org/10.1021/acscatal.5b02426.
[12] H.K. Luo, C. Wang, W. Rusli, C.Z. Li, E. Widjaja, P.K. Wong, L.P. Stubbs, M.V. Meurs, J. Organomet. Chem. 798 (2015) 354–366, https://doi.org/10.1016/j.jorganchem.2015.05.036.
[13] I. Bratko, M. Gomez, Dalton Trans. 42 (2013) 10664–10681, https://doi.org/10.1039/C3DT50963J.
[14] K. Lian, Y. Zhu, W. Li, S. Dai, C. Chen, Macromolecules 50 (2017) 6074–6080, https://doi.org/10.1021/acs.macromol.7b01087;
C. Zou, S. Dai, C. Chen, Macromolecules 51 (2018) 49–56, https://doi.org/10.1021/acs.macromol.7b02156.
[15] M. Khoshsefat, G.H. Zohuri, N. Ramezanian, S. Ahmadjo, M. Haghpanah, J. Polym. Sci. Part A Polym. Chem. 54 (2016) 3000–3011, https://doi.org/10.1002/pola.28186.
[16] F. Wang, R. Tanaka, Q. Li, Y. Nakayama, J. Yuan, T. Shiono, J. Mol. Catal. A Chem. 398 (2015) 231–240, https://doi.org/10.1016/j.molcata.2014.11.004.
[17] Z. Wang, R. Zhang, W. Zhang, G.A. Solan, Q. Liu, T. Liang, W.H. Sun, Catal. Sci. Technol. 9 (2019) 1933–1943, https://doi.org/10.1039/C9CY00293F.
[18] J. Guo, Z. Wang, W. Zhang, I.I. Oleynik, A. Vignesh, I.V. Oleynik, X. Hu, Y. Sun, W.H. Sun, Molecules 24 (2019) 1176, https://doi.org/10.3390/molecules24061176.
[19] A.A. Antonov, N.V. Semikolenova, E.P. Talsi, K.P. Bryliakov, J. Organomet. Chem. 884 (2019) 55–58, https://doi.org/10.1016/j.jorganchem.2019.02.002.
[20] L. Wang, J. Sun, Inorg. Chim. Acta 361 (2008) 1843–1849, https://doi.org/10.1016/j.ica.2007.09.039.
[21] B.K. Bahuleyan, K.J. Lee, S.H. Lee, Y. Liu, W. Zhou, I. Kim, Catal. Today 164 (2011) 80–87, https://doi.org/10.1016/j.cattod.2010.10.084.
[22] T. Sun, Q. Wang, Z. Fan, Polymer 51 (2010) 3091–3098, https://doi.org/10.1016/j.polymer.2010.04.050.
[23] Q. Xing, T. Zhao, S. Du, W. Yang, T. Liang, C. Redshaw, W. Sun, Organometallics 33 (2014) 1382–1388, https://doi.org/10.1021/om4010884.
[24] Q. Chen, W. Zhang, G.A. Solan, T. Liang, W.H. Sun, Dalton Trans. 47 (2018) 6124–6133, https://doi.org/10.1039/c8dt00907d.
[25] P. Barbaro, C. Bianchini, G. Giambastiani, I.G. Rios, A. Meli, W. Oberhauser, A.M. Segarra, L. Sorace, A. Toti, Organometallics 26 (2007) 4639–4651, https://doi.org/10.1021/om7005062.
[26] D. Takeuchi, S. Takano, Y. Takeuchi, K. Osakada, Organometallics 33 (2014) 5316–5323, https://doi.org/10.1021/om500629a.
[27] Q. Khamker, Y.D.M. Champouret, K. Singh, G.A. Solan, Dalton Trans. 41 (2009) 8935–8944, https://doi.org/10.1039/b910181k.
[28] A.P. Armitage, Y.D.M. Champouret, H. Grigoli, J.D.A. Pelletier, K. Singh, G.A. Solan, Eur. J. Inorg. Chem. 29 (2008) 4597–4607, https://doi.org/10.1002/ejic.200800650.
[29] C. Bianchini, G. Giambastiani, I.G. Rios, A. Meli, W. Oberhauser, L. Sorace, A. Toti, Organometallics 26 (2007) 5066–5078, https://doi.org/10.1021/om7006503.
[30] W.H. Sun, Q. Xing, J. Yu, E. Novikova, W. Zhao, X. Tang, T. Liang, C. Redshaw, Organometallics 32 (2013) 2309–2318, https://doi.org/10.1021/om301086p.
[31] S. Zhang, I. Vystorop, Z. Tang, W.H. Sun, Organometallics 26 (2007) 2456–2460, https://doi.org/10.1021/om070062z.
[32] Q. Chen, H. Suo, W. Zhang, R. Zhang, G.A. Solan, T. Liang, W.H. Sun, Dalton Trans. 48 (2019) 8264–8278, https://doi.org/10.1039/c9dt01235d.
[33] M. Khoshsefat, S. Ahmadjo, G. Zohuri, M.M. Mortazavi, J.B.P. Soares, New J. Chem. 42 (2018) 8334–8337, https://doi.org/10.1039/C8NJ01678J.
[34] M.A. Milani, D. González, R. Quijada, N.R.S. Basso, M.L. Cerrada, D.S. Azambuja, G.B. Galland, Compos. Sci. Technol. 84 (2013) 1–7, https://doi.org/10.1016/j.compscitech.2013.05.001.
[35] M. Khoshsefat, S. Ahmadjo, S.M.M. Mortazavi, G.H. Zohuri, RSC Adv. 6 (2016) 88625–88632, https://doi.org/10.1039/C6RA16243F.
[36] W. Collins, J. Seelenbinder, F. Higgins, Determination of the Vinyl Content of Polyethylene Resins, Agilent Technol Inc, US, 2012.
[37] G.H. Zohuri, S. Damavandi, E. Dianat, R. Sandaroos, Intern. J. Polym. Mater. 60 (2011) 37–41, https://doi.org/10.1080/00914037.2010.551362.
[38] M. Khoshsefat, N. Beheshti, G.H. Zohuri, S. Ahmadjo, S. Soleimanzadegan, Polym. Sci. Ser. B 58 (2016) 1–8, https://doi.org/10.1134/S1560090416050067.
[39] M. Kimiaghalam, H.N. Isfahani, G.H. Zohuri, A. Keivanloo, Appl. Organomet. Chem. 32 (2018) e4153, , https://doi.org/10.1002/aoc.4153.
[40] M. Mogheiseh, G.H. Zohuri, M. Khoshsefat, Macromol. React. Eng. 12 (2018) 1800006, https://doi.org/10.1002/mren.201800006.
[41] A. Dechal, M. Khoshsefat, S. Ahmadjo, S.M.M. Mortazavi, G.H. Zohuri, H. Abedini, 32 (2018) e4355. https://doi.org/10.1002/aoc.4355.
[42] M. Khoshsefat, A. Dechal, S. Ahmadjo, S.M.M. Mortazavi, G.H. Zohuri, J.B.P. Soares, New. J. Chem. 42 (2018) 18288–18296, https://doi.org/10.1039/c8nj04481c.